Research article

Journal of Applied Toxicology

Received: 6 July 2016, Revised: 17 July 2016, Accepted: 20 July 2016 Published online in Wiley Online Library: 24 August 2016

(wileyonlinelibrary.com) DOI 10.1002/jat.3376

RNA-sequencing analysis reveals the hepatotoxic mechanism of perfluoroalkyl alternatives, HFPO2 and HFPO4, following exposure in mice

Jianshe Wang, Xiaoyang Wang, Nan Sheng, Xiujuan Zhou, Ruina Cui, Hongxia Zhang and Jiayin Dai*

ABSTRACT: The toxicological impact of traditional perfluoroalkyl chemicals has led to the elimination and restriction of these substances. However, many novel perfluoroalkyl alternatives remain unregulated and little is known about their potential effects on environmental and human health. Daily administration of two alternative perfluoroalkyl substances, HFPO2 and HFPO4 (1 mg kg^{-1} body weight), for 28 days resulted in hepatomegaly and hepatic histopathological injury in mice, particularly in the HFPO4 group. We generated and compared high-throughput RNA-sequencing data from hepatic tissues in control and treatment group mice to clarify the mechanism of HFPO2 and HFPO4 hepatotoxicity. We identified 146 (101 upregulated, 45 downregulated) and 1295 (716 upregulated, 579 downregulated) hepatic transcripts that exhibited statistically significant changes (fold change ≥2 or ≤0.5, false discovery rate < 0.05) after HFPO2 and HFPO4 treatment, respectively. Among them, 111 (82 upregulated, 29 downregulated) transcripts were changed in both groups, and lipid metabolism associated genes were dominant. Thus, similar to their popular predecessors, HFPO2 and HFPO4 exposure exerted hepatic effects, including hepatomegaly and injury, and altered lipid metabolism gene levels in the liver, though HFPO4 exerted greater hepatotoxicity than HFPO2. The unregulated use of these emerging perfluoroalkyl alternatives may affect environmental and human health, and their biological effects need further exploration. Copyright © 2016 John Wiley & Sons, Ltd.

Additional supporting information may be found in the online version of this article at the publisher's web-site.

Keywords: HFPO2; HFPO4; Hepatotoxicity; RNA-seq; PPAR

Introduction

Primer information for qPCR is listed in Supplementary Table S1. The quality control of the liver RNA-seq results in mice after HFPO2 and HFPO4 treatment is listed in Supplementary Table S2. The mapping rates of the genomic sequence RNA-seq results are given in Supplementary Table S3. The significantly changed genes after HFPO2 and HFPO4 treatment are listed in Supplementary Table S4. The enriched GO terms of the differentially expressed hepatic sequences in mice after HFPO2 and HFPO4 treatment are listed in Supplementary Table S5. The significantly changed cytochrome P450 genes after HFPO2 and HFPO4 treatment are shown in Supplementary Table S6. Weight changes in male mice treated with HFPO2 and HFPO4 are shown in Supplementary Figure S1. The mean quality distribution of the RNA-seq results is shown in Supplementary Figure S2. The RPKM saturation is shown in Supplementary Figure S3. The volcano plot analysis of changes in transcript expression after HFPO2 and HFPO4 treatment is shown in Supplementary Figure S4. The heat map results of differentially expressed sequences after treatment are shown in Supplementary Figure S5.

Perfluoroalkyl substances (PFASs) are a class of highly stable manufactured compounds with varying lengths of fluorinated carbon backbones. Owing to their unique surface active properties associated with organic fluorocarbon chemistry, they are used in many industrial applications and consumer products, from stain- and water-resistant coatings for carpets and fabrics to fast-food containers, fire-resistant foams, paints and hydraulic fluids (Calafat *et al.*, 2007). The carbon-fluoride bonds that characterize PFASs also make them highly stable and environmentally persistent, resulting in their widespread detection in occupationally exposed populations (Olsen & Zobel, 2007), diverse general human populations (Fromme *et al.*, 2009; Kannan *et al.*, 2004; Karrman *et al.*, 2006), as well as in wildlife and environmental matrices in remote regions. Two of the most widely detected compounds are eight-carbon chain perfluorooctane sulfonate (PFOS) and perfluorooctanoic acid (PFOA) (Giesy & Kannan, 2001). Since 2000, the manufacturing practices for PFASs have changed considerably and the emissions of PFOS and PFOA have decreased (Lau *et al.*, 2007). In 2006, eight major producers of perfluorinated carboxylic acids, fluoropolymers and fluorotelomer substances joined the US EPA 2010/15 PFOA Stewardship Program to eliminate these long chain perfluorinated compounds and their potential precursors by 2015 (US EPA, 2006).

*Correspondence to: Jiayin Dai, Key Laboratory of Animal Ecology and Conservation Biology, Institute of Zoology, Chinese Academy of Sciences, Beijing, 100101, People's Republic of China.
E-mail: daijy@ioz.ac.cn

Key Laboratory of Animal Ecology and Conservation Biology, Institute of Zoology, Chinese Academy of Sciences, Beijing 100101, People's Republic of China

 Copyright © 2016 John Wiley & Sons, Ltd.

ED_002330_00119854-00001

However, many alternative chemicals with shorter or longer alkyl chains remain unregulated and continue to be released into the environment (Haug *et al.*, 2010; Ishibashi *et al.*, 2008; Jensen & Leffers, 2008; So *et al.*, 2006; Wang Z *et al.* 2013, Wang *et al.*, 2015a). Among them, the dimer acid of hexafluoropropylene oxide (HFPO2) was recently identified in environmental samples (Heydebreck *et al.*, 2015; Strynar *et al.*, 2012; Wang Z *et al.*, 2013). HFPO is a well-known versatile synthetic building block in the manufacture of fluoropolymers as well as a number of polyfluorinated and perfluorinated intermediates (Millauer *et al.*, 1985). The ammonium salt of HFPO2, namely GenX from DuPont, is used as a processing aid for fluoropolymer resin manufacturing (DuPont, 2010), and has been registered under REACH in Europe with an annual production volume of 10–100 tons (European Chemicals Agency [ECHA], 2015). The detection of HFPO2 in the environment could be due to residual leaching from commercial products or direct release during manufacturing processes (Wellington Reporter, 2013). HFPO tetramer (HFPO4) is the other oligomerization chemical of HFPO, though currently no data are available in regards to its annual production or distribution in environmental matrices.

The ubiquitous nature and persistence of PFASs in the environment and within the human body have led to efforts to understand the biological effects associated with exposure. Laboratory animal studies have shown that the PFAS exposure leads to loss of body weight, reduced cholesterol, increased liver weight, adenomas and many other toxicological hazards (Lau *et al.*, 2007; Frisbee *et al.*, 2010; Kennedy *et al.*, 2004). Animal studies have also indicated that some PFASs induce toxicological hazards via a peroxisome proliferator-activated receptor alpha (PPARα) agonistic mode in rodents (Kennedy *et al.*, 2004). Some epidemiological studies, mostly medical surveillance studies of male chemical workers, have shown that exposure to PFASs (PFOA and possibly PFOS) is modestly correlated with total cholesterol, low-density lipoprotein cholesterol and/or triglycerides (TG) in humans (Frisbee *et al.*, 2010; Olsen & Zobel 2007; Steenland *et al.*, 2009). Although hepatotoxicity of popular perfluoroalkyl acids (PFAAs), such as PFOS and PFOA, have been reported, little is currently known regarding whether HFPO2 and HFPO4 can exert negative health effects on animals and humans, except for a simple hazard description of HFPO2 given to the ECHA by the suppliers (ECHA, 2015). It should not be taken for granted that these alternatives are less or more hazardous to the environment and humans than their predecessors. Further studies are required, particularly with the application of next-generation sequencing technologies, which have dramatically accelerated genome-wide comparison of transcriptomes (Mortazavi *et al.*, 2008; Ozsolak & Milos, 2011; Sultan *et al.*, 2008; Wang Z *et al.*, 2009). In the present study, we investigated the effects and hazards of HFPO2 and HFPO4 exposure on mice livers, and explored the responses of hepatic transcripts following exposure using high-throughput RNA sequencing (RNA-seq).

Materials and methods

Chemicals and treatments

Both HFPO2 (2,3,3,3-tetrafluoro-2-(1,1,2,2,3,3,3-heptafluoro propoxy)propanoic acid, CAS number 62037–80-3, > 99% purity) and HFPO4 (propanoic acid,2,3,3,3-tetrafluoro-2-[1,1,2,3,3,3-hexafluoro-2-[1,1,2,3,3,3-hexafluoro-2-(1,1,2,2,3,3,3-heptafluoropro poxy)propoxy]propoxy] CAS number 65294–16-8, > 99% purity) were synthesized by Dr Yong Guo at the Shanghai Institute of Organic Chemistry, Chinese Academy of Sciences. The chemical structures of these two perfluoropolyethers are shown in Fig. 1. All other chemicals and reagents were of analytical grade. Male ICR mice (6–8 weeks of age) were purchased from the Weitong Lihua Laboratory Animal Central (Beijing, China) and maintained in a mass air-displacement room with a 12 h light–dark cycle at a temperature of 20–26 °C and a relative humidity of 50–70%. Animals had access to food and water *ad libitum*. After 1 week of acclimatization, the mice were randomly separated into three groups ($n = 12$ per group), i.e., the control, HFPO2 treatment group and HFPO4 treatment group. Both HFPO2 and HFPO4 were prepared in 0.5% Tween-20 (Beijing Chemical Reagent Co., Beijing, China). The chemicals were given orally via gavage to treatment group mice at doses of 1 mg kg^{-1} of body weight once a day for 4 weeks based on our pretest experiment. Control mice were treated similarly, but with the vehicle only. During exposure, the animals were weighed every 4 days. At the end of the experiment, all animals were fasted overnight and then weighed and killed by cervical dislocation. Livers were removed, weighed and cut into small pieces. Some pieces were fixed in 10% formalin for histopathological analysis, with the remaining pieces frozen in liquid nitrogen immediately and stored at −80 °C for HFPO2 and HFPO4 analysis and RNA extraction. Blood was collected, placed at room temperature to coagulate and then centrifuged at 2000 *g* for 15 min. Serum was then collected and stored at −80 °C until analysis. All experimental manipulations were undertaken according to protocols approved by the Animal Ethics Committee of the Institute of Zoology, Chinese Academy of Sciences.

Serum parameters and hepatic histopathological analysis

Standard spectrophotometric methods using a HITACHI-7170 A automatic analyzer (Hitachi Limited, Tokyo, Japan) were used to measure serum parameters, including alanine transaminase (ALT), aspartate aminotransferase (AST), TG and total cholesterol, etc. Formalin-fixed liver tissues were processed sequentially in ethanol, xylene and paraffin. Tissues were then embedded in paraffin wax, sectioned transversely at 4–5 μm, mounted on slides and stained with hematoxylin and eosin for histopathological observation.

RNA isolation, RNA-sequence library preparation and sequencing

Total RNA of mice livers (three samples in each group) was isolated using the RNeasy plus Mini Kit (Qiagen, Culver City, CA, USA) followed by DNaseI (Invitrogen, Life Technologies, Carlsbad, CA, USA) treatment according to the manufacturer's protocols. The total RNA was then sent out for a commercial sequencing in Annoroad Genomics (Beijing, China). Poly(A) mRNA was isolated

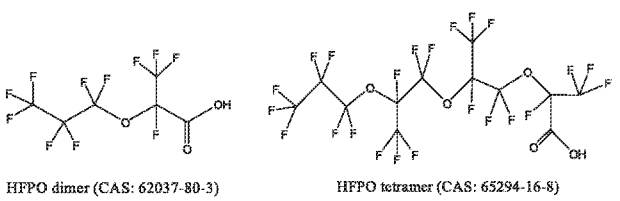

Figure 1. Chemical structure and CAS number of HFPO2 and HFPO4.

Copyright © 2016 John Wiley & Sons, Ltd.

from total RNA with oligo(dT) beads and then fragmented. The cleaved RNA fragments were transcribed into first-strand cDNA using reverse transcriptase and random hexamer primers, followed by second-strand cDNA synthesis in a reaction buffer, including dNTPs, DNA polymerase I and RNase H. The double-stranded cDNA was further subjected to end repair followed by a single A base addition. It was then ligated with an adaptor using T4 quick DNA ligase. Adaptor-ligated fragments were selected according to size and the desired range of cDNA fragments were excised from the gel. Polymerase chain reaction (PCR) was performed to selectively enrich and amplify the fragments. Finally, after validation on an Agilent 2100 Bioanalyzer (Agilent Technologies, Palo Alto, CA, USA), the cDNA library was sequenced on a flow cell using an Illumina HiSeq 2500 platform.

Mapping of reads and differential transcriptome analysis

The raw reads were cleaned by removing sequences in which more than five nucleotides were from the adaptor, and filtering the low-quality reads, including reads with unknown nucleotides >5%, and reads in which the percentage of low-quality bases ($Q \leq 19$) was >50%. The short reads were mapped to whole genome reference sequences with the TopHat program (Trapnell *et al.*, 2009). Transcript expression was calculated with RPKM (reads per kb per million mapped reads) (Mortazavi *et al.*, 2008) using the formula $RPKM = 10^6 R/(NL/10^3)$, where RPKM is the expression of Transcript A, R is the number of fragments that uniquely align to transcript A, N is the total number of fragments that uniquely align to all transcripts and L is the base number in the exon region of transcript A. The RPKM method can eliminate the influence of different gene lengths and sequencing levels on gene expression. Therefore, the calculated gene expression can be directly used for comparing the differences in gene expression between treatment and control groups. For transcript expression analysis, saturation and hierarchical cluster of the transcripts were also carried out. Differential transcription of each transcript was then tested between the control and treatment groups using the DEGseq program (Wang L *et al.*, 2010). False discovery rate (FDR) was used in the multiple hypothesis testing to correct the *P* value (Benjamini & Hochberg, 1995). In this study, we used the absolute value of $\log_2(RPKM_{treatment}/RPKM_{control}) \geq 1$ (fold change ≥2 or ≤0.5) and FDR < 0.05 as the thresholds for differentially expressed genes (DEGs) under treatment.

The DEGs were subjected to annotation and functional classification against databases, including the NCBI, Ensemble, gene ontology (GO) and Kyoto Encyclopedia of Genes and Genomes (KEGG) databases. Enrichment statistics were computed based on hypergeometric distribution and adjusted with the Benjamini–Yekutieli's multiple testing corrections (Benjamini & Yekutieli, 2001; Young *et al.*, 2010). The GO terms and KEGG pathways showing $q < 0.001$ were considered as significantly enriched in the treatment group compared with the control.

Quantitative polymerase chain reaction

We used quantitative PCR (qPCR) to confirm part of the RNA-seq DEGs after HFPO2 and HFPO4 treatment. Total RNAs from the livers of the control, HFPO2, and HFPO4 group mice were isolated using the RNeasy plus Mini Kit (Qiagen) followed by DNaseI (Invitrogen) treatment according to the manufacturer's protocols. cDNA was synthesized using an oligo(dT)15 primer and M-MLV reverse transcriptase (Promega, Madison, WI, USA). The cDNA was then used as a template in 25 μl reactions containing 12.5 μl of 2 × QuantiTect SYBR Green PCR master mix and 0.1 μM each of forward and reverse gene-specific primers, with 18S rRNA chosen as the internal control for normalization. Primer information is listed in Supplementary Table S1. The qPCR was performed with the Stratagene Mx3000P qPCR system (Stratagene, La Jolla, CA, USA) under the following conditions: denaturing at 95 °C for 2 min followed by 40 cycles of 15 s at 95 °C, 15 s at 58 °C, and 15 s at 72 °C. Melting curve analysis (60–95 °C) and gel electrophoresis were used for assessing amplification specificity. qPCR data were analyzed with MxPro qPCR software and the comparative C_T ($2^{-\Delta\Delta CT}$) method was used to calculate the fold change of their mRNA levels (Livak & Schmittgen, 2001).

Statistical analysis

All data were analyzed using SPSS for Windows 14.0 Software (SPSS, Inc., Chicago, IL, USA). All values are expressed as means ± SEM. The ratio of liver organ to body weight was calculated to yield relative liver weights. Body weight and relative liver weight were analyzed using one-way analysis of variance followed by Fisher's least significant difference test. Results were considered statistically significant at $P \leq 0.05$.

Results

Organ weights and serum parameters

There were no significant body weight changes observed between the treatment and control groups (Supplementary Fig. S1). However, the liver weights in the treatment groups increased significantly compared with that of the control group, showing an increase of 30.8% and 119.9% in the HFPO2 and HFPO4 groups, respectively ($P < 0.01$) (Table 1). Relative liver weights (hepatosomatic index) markedly increased by 28.1% and 123.3% in the HFPO2 and HFPO4 groups ($P < 0.01$), respectively. Serum ALT and AST, two transaminases that leak into the bloodstream when liver cells are damaged, increased in the HFPO4 group compared with that in the control. In addition, many other serum parameters associated with liver function were also changed significantly after HFPO2 and/or HFPO4 treatments, including an increase in lactate dehydrogenase, alkaline phosphatase and low-density lipoprotein cholesterol, and a decrease in total bilirubin and TG. These biochemical parameters changed more significantly in the HFPO4 group than those in the HFPO2 group when compared with the control, suggesting that hepatocytes were impaired more extensively in HFPO4-treated mice.

Hepatic histopathology

Mice exhibited hepatic histopathological injuries after exposure to HFPO2 and HFPO4 compared with that of the control. Lipid droplet accumulation, swollen hepatocytes and nuclei, mild steatosis and karyolysis were observed in the hepatocytes of mice exposed to HFPO2 and HFPO4 (Fig. 2A). Mice exposed to HFPO4 showed more severe hepatic histopathological changes than that of HFPO2-treated mice when compared with the control, with areas of hepatocytes undergoing focal necrosis. In addition, infiltration of inflammatory cells and vacuolar degeneration were both observed. Exposure to HFPO2 and HFPO4 elicited hepatocellular hypertrophy, particularly in the HFPO4 treatment group. As shown in Figure 2(B), the average number of cell nuclei within a definite area (1392 × 1040), as determined by InForm2.0.1 software, was

 Copyright © 2016 John Wiley & Sons, Ltd.

ED_002330_00119854-00003

Table 1. Body weight, liver weight and serum biochemistry parameters in male mice after HFPO2 and HFPO4 treatment

	Ctrl	HFPO2	HFPO4
Body weight (B)[a]	35.05 ± 0.52	35.74 ± 0.59	34.53 ± 0.69
Liver weight (L)	1.46 ± 0.03	1.91 ± 0.05**	3.21 ± 0.09**
Relative liver weight (L/B × 100%)	4.16 ± 0.09	5.33 ± 0.10**	9.29 ± 0.18**
ALT (IU l^{-1})	35.1 ± 2.57	41.8 ± 3.33	273.4 ± 34.59**
AST (IU l^{-1})	136.2 ± 11.71	149.9 ± 9.38	278.5 ± 22.6**
ALP (IU l^{-1})	106.8 ± 8.41	160.8 ± 17.38**	642.5 ± 95.86**
TBA (μmol l^{-1})	1.46 ± 0.12	1.39 ± 0.15	2.99 ± 0.49**
TBIL(μmol l^{-1})	0.78 ± 0.1	0.49 ± 0.11*	0.43 ± 0.07**
DBIL (μmol l^{-1})	0.71 ± 0.07	0.39 ± 0.05**	0.72 ± 0.1
TP (g l^{-1})	60.11 ± 0.92	58.37 ± 1.37	59.2 ± 1.4
ALB (IU l^{-1})	23.08 ± 0.33	22.91 ± 0.39	23.22 ± 0.33
TCHO (mmol l^{-1})	4.21 ± 0.18	4.43 ± 0.26	3.59 ± 0.29
TG (mmol l^{-1})	2.09 ± 0.21	1.9 ± 0.14	1.26 ± 0.09**
HDL-C (mmol l^{-1})	4.27 ± 0.16	4.31 ± 0.21	3.06 ± 0.24**
LDL-C (mmol l^{-1})	0.54 ± 0.04	0.81 ± 0.08**	0.81 ± 0.1*
LDH (mmol l^{-1})	1508.7 ± 107.25	1604.6 ± 57.14	2114.1 ± 41.29**
AFU (U l^{-1})	21.95 ± 0.45	21.39 ± 0.72	28.85 ± 1.69**

Parameters: AFU, α-L-fucosidase; ALB, albumin; ALP, alkaline phosphatase; ALT, alanine aminotransferase; AST, aspartate aminotransferase; DBIL, direct bilirubin; HDL-C, high-density lipoprotein cholesterol; IBIL, indirect bilirubin; LDH, lactate dehydrogenase; LDL-C, low-density lipoprotein cholesterol; TBA, total bile acid; TBIL, total bilirubin; TCHO, total cholesterol; TG, triglycerides; TP, total protein.

[a]Body weight after overnight fasting following HFPO2 and HFPO4 exposure. Mice were treated with HFPO2 or HFPO4 (1 mg kg^{-1} day^{-1}) for 28 days.

Results are presented as means ± SEM ($n = 10–11$).

* $P < 0.05$;

** $P < 0.01$ versus control.

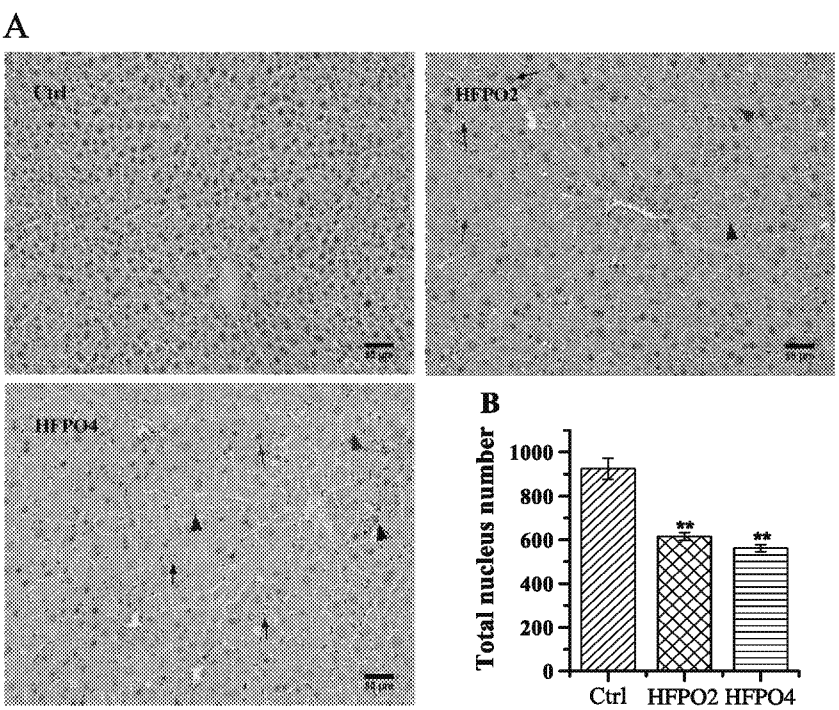

Figure 2. Hepatic histopathological results in mice after HFPO2 and HFPO4 treatment. Liver sections stained with hematoxylin and eosin (× 200) (A). Swollen hepatocytes (red arrow), swollen nucleus (black arrow), inclusion body (blue arrow), mild steatosis (red arrowhead), karyolysis (blue arrowhead) and necrosis (black arrowhead) are shown. Hepatocyte size alteration after HFPO2 and HFPO4 treatment (B). Average number of cell nuclei within a definite area (1392 × 1040) were calculated. Results are presented as means ± SEM ($n = 6$). *$P < 0.05$; **$P < 0.01$ versus control. Ctrl, control.

Copyright © 2016 John Wiley & Sons, Ltd.

sharply decreased in the treatment groups, with similar results also observed by manual counting (data not shown).

RNA-sequence data

The RNA transcripts from three samples in each group were deeply sequenced. A total of 155 485 511 paired-end reads were generated from the nine samples. The number of sequences from each sample ranged from 16.6 to 17.9 million. After removal of ambiguous nucleotides, low-quality sequences and adaptor sequences, a total of 154 614 854 clean reads (99.4%) were harvested for further analysis. Total clean nucleotides of the nine samples ranged from 8.3×10^8 to 8.9×10^8 nt, showing stability and consistency in sampling, library preparation, and sequencing. Detailed information on the quality control of RNA-seq is shown in Supplementary S2. The detailed information on mean quality distribution of nucleotides in the reads is shown in Supplementary Figure S2. The clean reads were then mapped to the genome sequences, with a mapping rate of 97–98% in all nine samples. Detailed information on genomic mapping, as well as exon, intron and intergenic mapping is shown in Supplementary Table S3.

Differentially expressed genes between treatment and control group

In exploring transcript changes between treatment and control groups, RPKM was adapted to eliminate the influence of variation in gene length and total read numbers. The saturation curves analysis of RPKM is shown in Supplementary Figure S3. Volcano plot analysis of the changes in transcript expression after HFPO2 and HFPO4 treatment is shown in Supplementary Figure S4. Using the threshold of FDR < 0.05 and absolute value of $\log_2$ (RPKM Ratio) ≥ 2, we identified 146 (101 upregulated, 45 downregulated) and 1295 (716 upregulated, 579 downregulated) hepatic transcripts as significantly changed genes after HFPO2 and HFPO4 treatment, respectively (Fig. 3). The heat map of differentially expressed sequences after treatment is shown in Supplementary Fig. S5. Among them, 111 (82 upregulated, 29 downregulated) transcripts were changed in both treatment groups, as listed in Supplementary Table S4.

Gene ontology terms and pathway enrichment of differentially expressed genes

Enrichment analysis of GO terms was further carried out for DEGs. After HFPO2 treatment, a high percentage of DEGs were assigned to "single-organism metabolic process," "small molecule metabolic process," "lipid metabolic process," "oxoacid metabolic process" and "regulation of immune system process" terms in biological process, "endoplasmic reticulum," "membrane region," "endoplasmic reticulum part," "endoplasmic reticulum membrane" and "nuclear outer membrane-endoplasmic reticulum membrane network" in cellular component, and "oxidoreductase activity," "monooxygenase activity," "arachidonic acid monooxygenase activity" and "arachidonic acid epoxygenase activity" in molecular function, respectively (Supplementary Table S5). For HFPO4, all significantly enriched GO terms reported for HFPO2 were included, though a broader profile of enriched GO terms was also found. Among KEGG pathway analysis of DEGs, 4 and 21 pathways were significantly enriched in HFPO2 and HFPO4 treatment groups, respectively, when compared with that in the control (Table 2). The pathways that changed in the HFPO2 treatment group included "PPAR signaling pathway," "arachidonic acid metabolism," "retinol metabolism" and "fatty acid degradation." All four pathways were associated with lipid metabolism and were found in the HFPO4 treatment group.

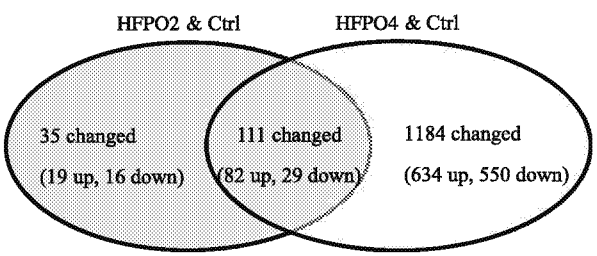

Figure 3. Venn diagram of differentially expressed sequences after HFPO2 and HFPO4 treatment. Ctrl, control.

Effect on hepatic peroxisome proliferator-activated receptor and cytochrome P450

The hepatic mRNA levels of PPAR targets, including CD36 antigen (Cd36), phospholipid transfer protein (Pltp), stearoyl-coenzyme A desaturase 1 (Scd1), acyl-coenzyme A oxidase 1, palmitoyl (Acox1), enoyl-coenzyme A, hydratase/3-hydroxyacyl coenzyme A dehydrogenase (Ehhadh), three cytochrome P450, family 4, subfamily a members (Cyp4a31, Cyp4a14 and Cyp4a32), adipocyte fatty acid-binding protein 4 (Fabp4) and solute carrier family 27 (fatty acid transporter, Slc27a1), were significantly increased after HFPO2 treatment (Fig. 4A). Moreover, many other genes in the PPAR pathway, such as liver fatty acid binding protein 1 (Fabp1), muscle carnitine palmitoyltransferase 1b (Cpt1b), Cpt2 and long chain acyl-coenzyme A dehydrogenase (Acadl), showed an increased tendency in HFPO2-treated livers compared with those in the control. The PPAR pathway was more strongly affected by HFPO4 than by HFPO2, not only in regards to the above upregulated PPAR-responsive genes in the HFPO2 group, which changed in the same direction after HFPO4 treatment, but also because many transcripts that showed a tendency of alteration ($P > 0.05$) after HFPO2 treatment were significantly changed after HFPO4 treatment. The upregulated transcripts included acetyl-coenzyme A acyltransferase 1B (Acaa1b), lipoprotein lipase (Lpl), Scd2, Acadl, acyl-CoA synthetase long chain family member 4 (Acsl4), apolipoprotein A-I (Apoa1), Fabp1, cytochrome P450, family 4, subfamily a, polypeptide 12B (Cyp4a12b), acyl-CoA synthetase long chain family member 3 (Acsl3), Cpt1b and cytosolic phosphoenolpyruvate carboxykinase (Pepck), whereas the downregulated transcripts included cytochrome P450, family 27, subfamily a, polypeptide 1 (Cyp27a1) (Fig. 4A). PPAR pathway genes, which were identified as significantly changed by RNA-seq in mice livers after both HFPO2 and HFPO4 exposure, were further validated by qPCR. All 10 PPAR pathway genes showed consistency or similar trends between RNA-seq and qPCR results (Fig. 4B).

HFPO4 affected a broader profile of pathways than HFPO2. Two pathways enriched by HFPO4 were "Drug metabolism-cytochrome P450 (map00982)" and "Metabolism of xenobiotics by cytochrome P450 (map00980)." In total, among the DEGs detected following HFPO4 treatment, 35 members of cytochrome P450 transcripts were included, while only nine members were altered by HFPO2 exposure (Supplementary S6). Some Cyp transcripts changed in the same direction after exposure to the two chemicals. For example, three Cyp4a members (Cyp4a31, Cyp4a32 and Cyp4a14) increased

Copyright © 2016 John Wiley & Sons, Ltd.

ED_002330_00119854-00005

Table 2. Enriched KEGG pathways of differentially expressed hepatic sequences in mice after HFPO2 and HFPO4 treatments

Map	*q* value		Name
	HFPO2	HFPO4	
map03320	9.49E-09	1.07E-12	PPAR signaling pathway
map00590	1.71E-05	5.16E-06	Arachidonic acid metabolism
map00830	1.71E-05	3.99E-14	Retinol metabolism
map00071	6.51E-05	5.16E-06	Fatty acid degradation
map03010		2.21E-30	Ribosome
map04610		1.50E-17	Complement and coagulation cascades
map00980		3.22E-15	Metabolism of xenobiotics by cytochrome P450
map00982		1.58E-12	Drug metabolism – cytochrome P450
map05204		3.29E-12	Chemical carcinogenesis
map04512		1.99E-08	ECM-receptor interaction
map00983		8.52E-07	Drug metabolism – other enzymes
map01040		8.99E-07	Biosynthesis of unsaturated fatty acids
map01100		1.12E-06	Metabolic pathways
map00140		3.21E-05	Steroid hormone biosynthesis
map05010		3.88E-05	Alzheimer's disease
map04066		5.11E-05	HIF-1 signaling pathway
map04974		9.08E-05	Protein digestion and absorption
map03040		0.000108	Spliceosome
map00062		0.000113	Fatty acid elongation
map00591		0.000183	Linoleic acid metabolism
map03013		0.00029	RNA transport

in both the HFPO2 and HFPO4 treatment groups. However, some Cyp showed the opposite changes between the two chemicals; for example, Cyp2c29 and Cyp2b10 decreased in the HFPO2-treated group, but increased in the HFPO4-treated group.

Discussion

Liver weight in the HFPO2 (1.91 g) and HFPO4 (3.21 g) treatment groups showed significant increases compared with that of the control (1.46 g), increasing by 30.8% and 119.9%, respectively. Hepatomegaly is one of the most dominant effects of PFAS exposure, and has been observed not only in rodents but also in monkeys (Berthiaume & Wallace, 2002; Kennedy, 1987; Seacat *et al.*, 2002). In our previous study, following six different treatment doses of PFOA (0, 0.31, 1.25, 2.25 and 5 mg kg^{-1} day^{-1}) for 28 days, the liver weights in exposed mice increased by 27.2% and 105.4% in the 0.31 and 1.25 mg kg^{-1} day^{-1} PFOA exposure groups, respectively (Yan *et al.*, 2014). Compared with the above results, more extensive hepatomegaly was induced by 1 mg kg^{-1} day^{-1} of HFPO2 or HFPO4 in the present study than by exposure to 0.31 and 1.25 mg kg^{-1} day^{-1} of PFOA, respectively. Mice exhibited hepatic histopathological lesions after exposure to HFPO2 and HFPO4 compared with that of the control, which included lipid droplet accumulation, hepatocyte swelling and necrosis, and infiltration of inflammatory cells. Furthermore, more focal hepatocyte necroses were observed in the HFPO4 than HFPO2 treatment group. Although no significant change was observed in the HFPO2 treatment group, serum ALT, AST and lactate dehydrogenase levels increased and TG levels decreased significantly in the HFPO4 group. In total, based on hepatomegaly, histopathological alteration and serum parameters, HFPO2 and HFPO4 exposure resulted in hepatotoxicity similar to that of popular PFASs. All of the above parameters indicate that HFPO4 is a more toxic fluorinated alternative than HFPO2.

There is strong evidence in laboratory animals that PFASs elicit many of their effects through PPARα (Abbott *et al.*, 2007; Cheung *et al.*, 2004; Kennedy *et al.*, 2004). By binding with peroxisome proliferator response elements in the promoter region of target genes, PPARα widely influences lipid catabolism processes, including peroxisomal and mitochondrial β-oxidation pathways, fatty acid uptake, TG catabolism, and lipoprotein assembly and transport (Ijpenberg *et al.*, 1997; Kersten *et al.*, 2000). Cell-based assays using various binding and reporter constructs have also shown significant activation of PPARα by PFASs (Maloney & Waxman, 1999; Shipley *et al.*, 2004; Takacs & Abbott, 2007; Vanden Heuvel *et al.*, 2006). Using PPAR knockout mice, Rosen *et al.* (2008) found that 85% of the genes altered after 7 days of exposure to PFOA were dependent on PPARα; however, the subset of lipid homeostasis genes, which showed increased expression in PPARα-null mice, might be partly due to PPARγ and other transcriptional regulation factors, such as constitutively activated androstane receptor (Rosen *et al.*, 2008). PPARγ is a key regulator of lipid storage, adipocyte differentiation and inflammation control (Berger & Moller, 2002), but it is normally expressed at very low levels in the liver (Gavrilova *et al.*, 2003). Similar to popular PFASs, prominent hepatomegaly and perturbation of lipid metabolism associated genes were observed in mice treated with HFPO2 and HFPO4 in our study. Many genes involved in the PPAR pathway, including Cd36, Pltp, Acox1, Ehhadh, Cyp4a members and Slc27a1 in the HFPO2 and HFPO4 groups, and Acaa1b, Lpl, Scd2, Acadl, Acsl4, Apoa1, Pepck, Fabp1, Cyp4a12b and Cpt1b in the HFPO4 group only, were significantly increased. Among them, Acox1 is a rate-limiting enzyme in peroxisomal fatty acids β-oxidation and Cyp4a enzymes are involved in the ω-hydroxylate the terminal carbon of fatty acids (Johnson *et al.*, 1996; Lee *et al.*, 2004). The induction of these PPAR response genes demonstrated that HFPO2 and HFPO4 enhanced fatty acid oxidation in the liver similar to that of their predecessors, such as PFOA (Guruge *et al.*, 2006). Previous

 Copyright © 2016 John Wiley & Sons, Ltd.

ED_002330_00119854-00006

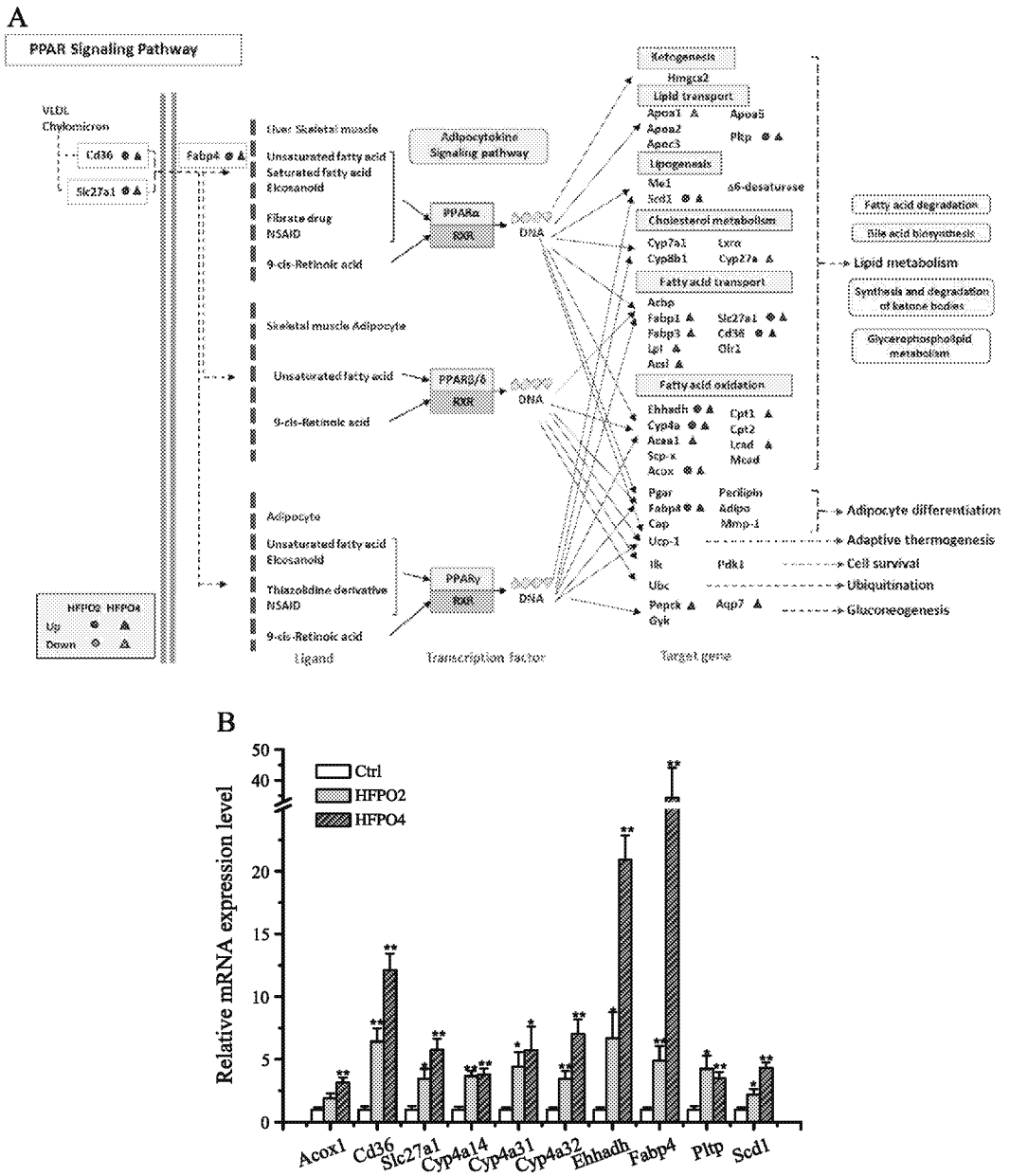

Figure 4. PPAR pathway. Changed PPAR pathway genes after HFPO2 and HFPO4 treatment (A). Significantly changed genes after HFPO2 and HFPO4 treatment are labeled with a circle and triangle, respectively. Upregulated genes are labeled in red and downregulated genes are labeled in blue. Quantitative polymerase chain reaction confirmation for PPAR pathway genes changed after HFPO2 and HFPO4 treatment (B). Results are presented as means ± SEM ($n = 6$). $^{*}P < 0.05$; $^{**}P < 0.01$ versus control. NSAID, non-steroidal anti-inflammatory drug; PPAR, peroxisome proliferator-activated receptor; RXR, retinoid X receptor; VLDL, very low-density lipoprotein.

publications indicate that PFASs significantly induce the activity of lipogenic enzymes, including Scd1, the rate-limiting enzyme in the biosynthesis of mono-unsaturated fatty acids (Kawashima *et al.*, 1989; Yamamoto & Kawashima, 1997). In the present study, the Scd1 mRNA levels increased markedly increased in in both the HFPO2- and HFPO4-treated groups, and HFPO4 also induced the expression of its isoform Scd2. Our previous study also showed that lipogenesis was activated in mice livers after PFNA exposure (Wang *et al.*, 2015b). The alteration of both lipogenesis and oxidation genes indicates that the perturbation effects of these alternative chemicals are similar to those of the traditional PFASs.

The Cyp play a central role in the detoxification of xenobiotics and the metabolism of endogenous compounds (Nebert & Russell, 2002; Nelson *et al.*, 1996, 2004). Many Cyps are reportedly altered following exposure to PFASs (Hu *et al.*, 2005; Yeung *et al.*, 2007). Cyp4a enzymes, which are involved in unsaturated fatty acid ω-oxidation, increased after HFPO2 and HFPO4 treatment. Many other Cyps were also changed after HFPO2 and HFPO4 treatment, particularly in the HFPO4-treated group. For example, Cyp2c29 and Cyp2b10, two members from the Cyp2 subfamily, showed opposite changes in the HFPO2 and HFPO4 treatment groups. Based on nuclear receptor gene knockout mice models, PPARα and constitutively activated androstane receptor have been suggested to play central roles in the induction of Cyps, including Cyp2b10, 3a11 and 4a14, after PFDA and PFOA exposure (Cheng & Klaassen, 2008).

Copyright © 2016 John Wiley & Sons, Ltd.

ED_002330_00119854-00007

Evidence suggests that the effects of PFAAs are closely correlated with carbon chain length (Liao *et al.*, 2009; Weiss *et al.*, 2009). Using human liver cell line HL-7702, our earlier research suggested that the inhibition effect on cell viability is stronger when PFAA carbon chain lengths are longer (Hu *et al.*, 2014). The transcriptional activation of peroxisome proliferation genes in primary rat hepatocytes by PFAAs is also reported as related to the length of each compound's carbon chain (Bjork & Wallace, 2009). Similar to their predecessors, the HFPO2 and HFPO4 perfluoroalkyl alternatives exerted hepatotoxicity, with the longer carbon chained HFPO4 exerting greater hepatotoxicity than that of HFPO2. Currently, the unregulated usage of these chemicals could lead to environmental hazards and health effects, and a more detailed safety assessment is needed.

Acknowledgements

We sincerely thank Dr. Yong Guo from the Shanghai Institute of Organic Chemistry, Chinese Academy of Sciences for providing HFPO4. This work was supported by the National Basic Research Program of China (973, grant no. 2013CB945004) and the Natural Science Foundation of China (grant no. 21477126).

Conflict of interest

The authors did not report any conflict of interest.

References

Abbott BD, Wolf CJ, Schmid JE, Das KP, Zehr RD, Helfant L, Nakayama S, Lindstrom AB, Strynar MJ, Lau C. 2007. Perfluorooctanoic acid induced developmental toxicity in the mouse is dependent on expression of peroxisome proliferator activated receptor-alpha. *Toxicol. Sci.* **98**: 571–581.

Benjamini Y, Hochberg Y. 1995. Controlling the false discovery rate – a practical and powerful approach to multiple testing. *J. R. Stat. Soc. Series B Stat. Methodol.* **57**: 289–300.

Benjamini Y, Yekutieli D. 2001. The control of the false discovery rate in multiple testing under dependency. *Ann. Stat.* **29**: 1165–1188.

Berger J, Moller DE. 2002. The mechanisms of action of PPARs. *Annu. Rev. Med.* **53**: 409–435.

Berthiaume J, Wallace KB. 2002. Perfluorooctanoate, perflourooctanesulfonate, and N-ethyl perfluorooctanesulfonamido ethanol; peroxisome proliferation and mitochondrial biogenesis. *Toxicol. Lett.* **129**: 23–32.

Bjork JA, Wallace KB. 2009. Structure–activity relationships and human relevance for perfluoroalkyl acid-induced transcriptional activation of peroxisome proliferation in liver cell cultures. *Toxicol. Sci.* **111**: 89–99.

Calafat AM, Wong LY, Kuklenyik Z, Reidy JA, Needham LL. 2007. Polyfluoroalkyl chemicals in the U.S. population: data from the National Health and Nutrition Examination Survey (NHANES) 2003-2004 and comparisons with NHANES 1999-2000. *Environ. Health Perspect.* **115**: 1596–1602.

Cheng X, Klaassen CD. 2008. Perfluorocarboxylic acids induce cytochrome P450 enzymes in mouse liver through activation of PPAR-alpha and CAR transcription factors. *Toxicol. Sci.* **106**: 29–36.

Cheung C, Akiyama TE, Ward JM, Nicol CJ, Feigenbaum L, Vinson C, Gonzalez FJ. 2004. Diminished hepatocellular proliferation in mice humanized for the nuclear receptor peroxisome proliferator-activated receptor alpha. *Cancer Res.* **64**: 3849–3854.

DuPont. 2010. GenX processing aid for making fluoropolymer resins. http://www2.dupont.com/Industrial_Bakery_Solutions/en_GB/assets/downloads/DuPont_GenX_Brochure_Final_07July2010.pdf.

ECHA ECA. 2015. Committee for Risk Assessment (RAC) Committee for Socio-economic Analysis (SEAC) Background document to the Opinion on the Annex XV dossier proposing restrictions on Perfluorooctanoic acid (PFOA), PFOA salts and PFOA-related substances. http://echa.europa.eu/documents/10162/13641/rest_pfoa_draftbd_en.pdf.

Frisbee SJ, Shankar A, Knox SS, Steenland K, Savitz DA, Fletcher T, Ducatman AM. 2010. Perfluorooctanoic acid, perfluorooctanesulfonate, and serum lipids in children and adolescents. *Arch. Pediatr. Adolesc. Med.* **164**: 860–869.

Fromme H, Tittlemier SA, Volkel W, Wilhelm M, Twardella D. 2009. Perfluorinated compounds – exposure assessment for the general population in Western countries. *Int. J. Hyg. Environ. Health* **212**: 239–270.

Gavrilova O, Haluzik M, Matsusue K, Cutson JJ, Johnson L, Dietz KR, Nicol CJ, Vinson C, Gonzalez FJ, Reitman ML. 2003. Liver peroxisome proliferator-activated receptor gamma contributes to hepatic steatosis, triglyceride clearance, and regulation of body fat mass. *J. Biol. Chem.* **278**: 34268–34276.

Giesy JP, Kannan K. 2001. Global distribution of perfluorooctane sulfonate in wildlife. *Environ. Sci. Technol.* **35**: 1339–1342.

Guruge KS, Yeung LW, Yamanaka N, Miyazaki S, Lam PK, Giesy JP, Jones PD, Yamashita N. 2006. Gene expression profiles in rat liver treated with perfluorooctanoic acid (PFOA). *Toxicol. Sci.* **89**: 93–107.

Haug LS, Thomsen C, Brantsaeter AL, Kvalem HE, Haugen M, Becher G, Alexander J, Meltzer HM, Knutsen HK. 2010. Diet and particularly seafood are major sources of perfluorinated compounds in humans. *Environ. Int.* **36**: 772–778.

Heydebreck F, Tang J, Xie Z, Ebinghaus R. 2015. Alternative and legacy perfluoroalkyl substances: differences between European and Chinese river/estuary systems. *Environ. Sci. Technol.* **49**: 8386–8395.

Hu J, Li J, Wang J, Zhang A, Dai J. 2014. Synergistic effects of perfluoroalkyl acids mixtures with J-shaped concentration-responses on viability of a human liver cell line. *Chemosphere* **96**: 81–88.

Hu W, Jones PD, Celius T, Giesy JP. 2005. Identification of genes responsive to PFOS using gene expression profiling. *Environ. Toxicol. Pharmacol.* **19**: 57–70.

Upenberg A, Jeannin E, Wahli W, Desvergne B. 1997. Polarity and specific sequence requirements of peroxisome proliferator-activated receptor (PPAR)/retinoid X receptor heterodimer binding to DNA. A functional analysis of the malic enzyme gene PPAR response element. *J. Biol. Chem.* **272**: 20108–20117.

Ishibashi H, Iwata H, Kim EY, Tao L, Kannan K, Amano M, Miyazaki N, Tanabe S, Batoev VB, Petrov EA. 2008. Contamination and effects of perfluorochemicals in Baikal seal (*Pusa sibirica*). 1. Residue level, tissue distribution, and temporal trend. *Environ. Sci. Technol.* **42**: 2295–2301.

Jensen AA, Leffers H. 2008. Emerging endocrine disrupters: perfluoroalkylated substances. *Int. J. Androl.* **31**: 161–169.

Johnson EF, Palmer CN, Griffin KJ, Hsu MH. 1996. Role of the peroxisome proliferator-activated receptor in cytochrome P450 4 A gene regulation. *FASEB J.* **10**: 1241–1248.

Kannan K, Corsolini S, Falandysz J, Fillmann G, Kumar KS, Loganathan BG, Mohd MA, Olivero J, Van Wouwe N, Yang JH, Aldoust KM. 2004. Perfluorooctanesulfonate and related fluorochemicals in human blood from several countries. *Environ. Sci. Technol.* **38**: 4489–4495.

Karrman A, Mueller JF, van Bavel B, Harden F, Toms LM, Lindstrom G. 2006. Levels of 12 perfluorinated chemicals in pooled Australian serum, collected 2002-2003, in relation to age, gender, and region. *Environ. Sci. Technol.* **40**: 3742–3748.

Kawashima Y, Uy-Yu N, Kozuka H. 1989. Sex-related differences in the enhancing effects of perfluoro-octanoic acid on stearoyl-CoA desaturase and its influence on the acyl composition of phospholipid in rat liver. Comparison with clofibric acid and tiadenol. *Biochem. J.* **263**: 897–904.

Kennedy GL, Jr. 1987. Increase in mouse liver weight following feeding of ammonium perfluorooctanoate and related fluorochemicals. *Toxicol. Lett.* **39**: 295–300.

Kennedy GL, Butenhoff JL, Olsen GW, O'Connor JC, Seacat AM, Perkins RG, Biegel LB, Murphy SR, Farrar DG. 2004. The toxicology of perfluorooctanoate. *Crit. Rev. Toxicol.* **34**: 351–384.

Kersten S, Desvergne B, Wahli W. 2000. Roles of PPARs in health and disease. *Nature* **405**: 421–424.

Lau C, Anitole K, Hodes C, Lai D, Pfahles-Hutchens A, Seed J. 2007. Perfluoroalkyl acids: a review of monitoring and toxicological findings. *Toxicol. Sci.* **99**: 366–394.

Lee GY, Kim NH, Zhao ZS, Cha BS, Kim YS. 2004. Peroxisomal-proliferator-activated receptor alpha activates transcription of the rat hepatic malonyl-CoA decarboxylase gene: a key regulation of malonyl-CoA level. *Biochem. J.* **378**: 983–990.

Liao C, Wang T, Cui L, Zhou Q, Duan S, Jiang G. 2009. Changes in synaptic transmission, calcium current, and neurite growth by perfluorinated compounds are dependent on the chain length and functional group. *Environ. Sci. Technol.* **43**: 2099–2104.

Copyright © 2016 John Wiley & Sons, Ltd.

Livak KJ, Schmittgen TD. 2001. Analysis of relative gene expression data using real-time quantitative PCR and the $2^{-\Delta\Delta CT}$ method. *Methods* **25**: 402–408.

Maloney EK, Waxman DJ. 1999. *trans*-Activation of PPARα and PPARγ by structurally diverse environmental chemicals. *Toxicol. Appl. Pharmacol.* **161**: 209–218.

Millauer H, Schwertfeger W, Siegemund G. 1985. Hexafluoropropene oxide – a key compound in organofluorine chemistry. *Angew. Chem. Int. Ed.* **24**: 161–179.

Mortazavi A, Williams BA, McCue K, Schaeffer L, Wold B. 2008. Mapping and quantifying mammalian transcriptomes by RNA-Seq. *Nat. Methods* **5**: 621–628.

Nebert DW, Russell DW. 2002. Clinical importance of the cytochromes P450. *Lancet* **360**: 1155–1162.

Nelson DR, Koymans L, Kamataki T, Stegeman JJ, Feyereisen R, Waxman DJ, Waterman MR, Gotoh O, Coon MJ, Estabrook RW, Gunsalus IC, Nebert DW. 1996. P450 superfamily: update on new sequences, gene mapping, accession numbers and nomenclature. *Pharmacogenetics* **6**: 1–42.

Nelson DR, Zeldin DC, Hoffman SM, Maltais LJ, Wain HM, Nebert DW. 2004. Comparison of cytochrome P450 (CYP) genes from the mouse and human genomes, including nomenclature recommendations for genes, pseudogenes and alternative-splice variants. *Pharmacogenetics* **14**: 1–18.

Olsen GW, Zobel LR. 2007. Assessment of lipid, hepatic, and thyroid parameters with serum perfluorooctanoate (PFOA) concentrations in fluorochemical production workers. *Int. Arch. Occup. Environ. Health* **81**: 231–246.

Ozsolak F, Milos PM. 2011. RNA sequencing: advances, challenges and opportunities. *Nat. Rev. Genet.* **12**: 87–98.

Rosen MB, Lee JS, Ren H, Vallanat B, Liu J, Waalkes MP, Abbott BD, Lau C, Corton JC. 2008. Toxicogenomic dissection of the perfluorooctanoic acid transcript profile in mouse liver: evidence for the involvement of nuclear receptors PPAR alpha and CAR. *Toxicol. Sci.* **103**: 46–56.

Seacat AM, Thomford PJ, Hansen KJ, Olsen GW, Case MT, Butenhoff JL. 2002. Subchronic toxicity studies on perfluorooctanesulfonate potassium salt in cynomolgus monkeys. *Toxicol. Sci.* **68**: 249–264.

Shipley JM, Hurst CH, Tanaka SS, DeRoos FL, Butenhoff JL, Seacat AM, Waxman DJ. 2004. *trans*-Activation of PPARα and induction of PPARα target genes by perfluorooctane-based chemicals. *Toxicol. Sci.* **80**: 151–160.

So MK, Yamashita N, Taniyasu S, Jiang Q, Giesy JP, Chen K, Lam PK. 2006. Health risks in infants associated with exposure to perfluorinated compounds in human breast milk from Zhoushan, China. *Environ. Sci. Technol.* **40**: 2924–2929.

Steenland K, Jin CF, MacNeil J, Lally C, Ducatman A, Vieira V, Fletcher T. 2009. Predictors of PFOA levels in a community surrounding a chemical plant. *Environ. Health Perspect.* **117**: 1083–1088.

Strynar, MJ, Dagnino, Lindstrom A, Andersen E, McMillan L, Thurman M, Ferrer I, Ball C. 2012. Identification of novel polyfluorinated compounds in natural waters using accurate mass TOFMS. 33rd SETAC North America Annual Meeting, Long Beach, USA, November 11–15.

Sultan M, Schulz MH, Richard H, Magen A, Klingenhoff A, Scherf M, Seifert M, Borodina T, Soldatov A, Parkhomchuk D, Schmidt D, OKeeffe S, Haas S, Vingron M, Lehrach H, Yaspo ML. 2008. A global view of gene activity and alternative splicing by deep sequencing of the human transcriptome. *Science* **321**: 956–960.

Takacs ML, Abbott BD. 2007. Activation of mouse and human peroxisome proliferator-activated receptors (alpha, beta/delta, gamma) by perfluorooctanoic acid and perfluorooctane sulfonate. *Toxicol. Sci.* **95**: 108–117.

Trapnell C, Pachter L, Salzberg SL. 2009. TopHat: discovering splice junctions with RNA-Seq. *Bioinformatics* **25**: 1105–1111.

US EPA. 2006. 2010/2015 PFOA Stewardship Program. https://www.epa.gov/assessing-and-managing-chemicals-under-tsca/fact-sheet-20102015-pfoa-stewardship-program.

Vanden Heuvel JP, Thompson JT, Frame SR, Gillies PJ. 2006. Differential activation of nuclear receptors by perfluorinated fatty acid analogs and natural fatty acids: a comparison of human, mouse, and rat peroxisome proliferator-activated receptor-α, −β, and -γ, liver X receptor-β, and retinoid X receptor-α. *Toxicol. Sci.* **92**: 476–489.

Wang J, Yan S, Zhang W, Zhang H, Dai J. 2015b. Integrated proteomic and miRNA transcriptional analysis reveals the hepatotoxicity mechanism of PFNA exposure in mice. *J. Proteome Res.* **14**: 330–341.

Wang L, Feng Z, Wang X, Wang X, Zhang X. 2010. DEGseq: an R package for identifying differentially expressed genes from RNA-seq data. *Bioinformatics* **26**: 136–138.

Wang Z, Gerstein M, Snyder M. 2009. RNA-Seq: a revolutionary tool for transcriptomics. *Nat. Rev. Genet.* **10**: 57–63.

Wang Z, Cousins IT, Scheringer M, Hungerbuhler K. 2013. Fluorinated alternatives to long-chain perfluoroalkyl carboxylic acids (PFCAs), perfluoroalkane sulfonic acids (PFSAs) and their potential precursors. *Environ. Int.* **60**: 242–248.

Wang Z, Cousins IT, Scheringer M, Hungerbuehler K. 2015a. Hazard assessment of fluorinated alternatives to long-chain perfluoroalkyl acids (PFAAs) and their precursors: status quo, ongoing challenges and possible solutions. *Environ. Int.* **75**: 172–179.

Weiss JM, Andersson PL, Lamoree MH, Leonards PE, van Leeuwen SP, Hamers T. 2009. Competitive binding of poly- and perfluorinated compounds to the thyroid hormone transport protein transthyretin. *Toxicol. Sci.* **109**: 206–216.

Wellington Reporter. 2013. New products: native and mass-labelled hexafluoropropylene oxide dimer acid. http://www.campro.eu/PDF/Brochures/Flyer-WELLINGTON/2013-20-Feb-Hexafluoropropylene-oxide.pdf.

Yamamoto A, Kawashima Y. 1997. Perfluorodecanoic acid enhances the formation of oleic acid in rat liver. *Biochem. J.* **325**: 429–434.

Yan S, Wang J, Zhang W, Dai J. 2014. Circulating microRNA profiles altered in mice after 28 d exposure to perfluorooctanoic acid. *Toxicol. Lett.* **224**: 24–31.

Yeung LW, Guruge KS, Yamanaka N, Miyazaki S, Lam PK. 2007. Differential expression of chicken hepatic genes responsive to PFOA and PFOS. *Toxicology* **237**: 111–125.

Young MD, Wakefield MJ, Smyth GK, Oshlack A. 2010. Gene ontology analysis for RNA-seq: accounting for selection bias. *Genome Biol.* **11**: R14.

Supporting information

Additional supporting information may be found in the online version of this article at the publisher's web site.

Copyright © 2016 John Wiley & Sons, Ltd.

ED_002330_00119854-00009